UDC 629.5.035:534-14

Branko BAJIĆ[1]
Jadranka TASIĆ[1]
Adil DŽUBUR[2]
Ivica JOVANOVIĆ[3]
Ratko DONESKI[1]

Authors' addresses:
[1] *Brodarski Institute - Marine Research & Special Technologies d.o.o.*, Zagreb, CROATIA
[2] formerly with[1], now with *VAMS d.o.o.*, Zagreb, CROATIA
[3] formerly with[1], now with *PELSYS d.o.o.*, Zagreb, CROATIA

Contact address:
B. Bajić, *Brodarski Institute*,
Av. V. Holjevca 20, 10020 Zagreb, CROATIA
Tel.: +385 1 / 65 04 379
Fax: +385 1 / 65 04 360
E-mail: bajic@zg.tel.hr
http://home.t-online.de/home/bajic

Received: 1998-03-13
Accepted: 1998-04-28

Propeller Hydroacoustic Noise - Review of Research at the Brodarski Institute*

Review

Basic results obtained from the research into screw propeller hydroacoustic noise at the Brodarski Institute in the seventies and eighties are presented. Cavitation, rotation, and vortex noise, and propeller singing are considered. The results relate to full- and model-scale, as well as empirical and theoretical models.

Key words: *hydroacoustics, propeller noise, cavitation*

Hidroakustički šum vijka - Pregled istraživanja u Brodarskom institutu

Pregledni rad

Prikazani su osnovni rezultati istraživanja hidroakustičkog šuma vijčanih propelera tijekom sedamdesetih i osamdesetih godina u Brodarskom institutu. Obuhvaćeni su kavitacijski, rotacijski i vrtložni šum te zujanje vijka. Riječ je o rezultatima vezanim na narav i modele, te empirijsko i matematičko modeliranje.

Ključne riječi: *hidroakustika, šum vijka, kavitacija*

Motivated by the development of several classes of submarines and submersibles, research and practical activity in the field of propeller hydroacoustic noise was continually under way at the Brodarski Institute in the seventies and eighties. The first author had initiated the activity and was leading the research team. Due to specific circumstances, this work was planned, organised, and realised with only sparse contact to other laboratories and researchers in the East or West. In 1992 the results were presented to German specialists at the Fraunhofer Research Group for Hydroacoustics in Ottobrunn, the Hamburg Ship Model Basin, and the Committee for Noise Reduction Onboard Ships of the German Navy. The approach has been recognised for several unique results based on the use of advanced measurement and signal processing methods, which have produced useful deviation from the mainstream of Western research.

The methodologies developed are reviewed here so that they can be more widely used. Four types of propeller hydroacoustic noise are considered: cavitation, rotation, vortex and propeller singing. Brief comments are given on a number of particular issues. If no other explicit references are given, the results were produced by the Brodarski Institute team. More detailed information on the results can be found in the published papers listed in the attached bibliography and in several hundred technical reports of the Brodarski Institute.

* The authorship of the findings presented here is shared between the five authors listed and a number of their colleagues and co-workers: Vladislav Komeštik, Zoran Saje, Alojz Hren, Stjepan Klak, Vili Tomac, Davor Blažević, Dubravko Kelenc, Goran Pavić, Damir Barić, Cvitan Jović, Olga Vernić, Goran Repanić, and Borut Aparnik.

1. Logical frame [29]

The basic task of propeller noise measurements, on model- and full-scale, and of propeller noise theoretical modelling is to estimate far free-field characteristics of various sources of propeller noise and to analyse the contributions of different parts of a propeller and the surrounding water volume to the total acoustic field. Spatial resolution of the noise source is of particular importance in case of cavitation noise. Two types of hydroacoustic models can be used to represent the propeller in such a description:

(a) Reduction of the propeller to an equivalent point source.

(b) Considering the propeller and its water surroundings to be a spatially-distributed noise source.

A good format for the (a)-type model is the power spectrum density (PSD) of the unit-distance free far acoustic field, while the volume density of this function (VDPSD) is appropriate for the (b)-type model. The PSD is a function of only noise frequency and propeller angular position, while the VDPSD additionally depends on the spatial co-ordinates within the distributed source volume.

Two cylindrical co-ordinate systems are convenient for propeller issues: one rotating with the propeller, $(r; \theta, z)$, and one nonrotating but coaxial with the propeller, $(r; \phi, z)$. The radial co-ordinates, r, measured from the propeller axis, and the axial ones, z, measured from the propeller plane along the propeller axis, are identical in the two systems. The angular co-ordinates, θ and ϕ, are measured in the propeller plane; the angles $\phi=0$ and $\theta=0$ coincide when the propeller is in a reference position. The co-ordinate ϕ quantifies the instantaneous angular position of the propeller, and θ specifies the physical

location on the propeller body. The basic propeller noise description - the VDPSD related to the point (r, θ, z) under the condition that the propeller lies in the angular position ϕ - can thus be written as $G(f; r, \theta, z; \phi)$, where f is noise frequency.

The (a)/(b)-PSD/VDPSD concept just described is consistent with four types of propeller noise descriptions. One is an estimate in the form of:

$$G(f; r, \theta, z; \phi) \quad \ldots f, r, \theta, z, \phi \tag{1}$$

as a function of the five variables listed. The three other descriptions yield estimates as functions of four, two and one variable, respectively:

$$<G(f; r, \theta, z; \phi)>_{\phi} \quad \ldots f, r, \theta, z, \tag{2}$$

$$\Sigma\{G(f; r, \theta, z; \phi)\}_{r,\theta,z} \quad \ldots f, \phi, \tag{3}$$

$$<\Sigma\{G(f; r, \theta, z; \phi)\}_{r,\theta,z}>_{\phi} \quad \ldots f. \tag{4}$$

Here $<>_{\phi}$ denotes averaging over $\phi \in [0,2\pi]$, and $\Sigma\{\}_{r,\theta,z}$ stands for integration over $(r,\theta,z) \in V$, where V is the volume occupied by the noise source.

Obviously, (1) yields the most detailed spectral description of the source. It specifies the source's spatial distribution as a function of the propeller position. The other forms are more restrictive. Form (2) reveals the contributions of different spatial elements of the propeller and its surroundings. These values are, however, averaged circumferentially. Form (3) yields the total propeller noise as a function of the propeller angular position, while (4) is simply the mean total propeller noise spectrum. Models of the (a) type are appropriately described by type (3) and (4) PSD functions while (b) types are describable by the VDPSD functional forms (1) and (2).

This classification of the propeller noise descriptions can be extended to include source directivity. A variation that often proves useful is reducing the spectral description to the data related to a suitable frequency band.

2. Cavitation noise

2.1 Sensors [15, 26]

Examples of sensory devices developed and used in the Brodarski Institute for the measurement of cavitation noise from model propeller are shown in Fig. 1. These include high frequency pressure transducers flush mounted in the window of the cavitation tunnel measuring section (a), streamlined holders with externally (b,c) or internally (d) mounted miniature hydrophones, carefully designed streamlined hydrophone (e), and water filled chambers (f) with acoustically transparent windows (g) attached to one or two sides of the tunnel measuring section. In the chambers, unlined or lined with absorbing rubber (h), simple sensors, arrays of sensors and elliptic reflectors (i) are used. The signals from these sensors, processed by suitable signal processing equipment, form the basis for all four types of measurements specified above.

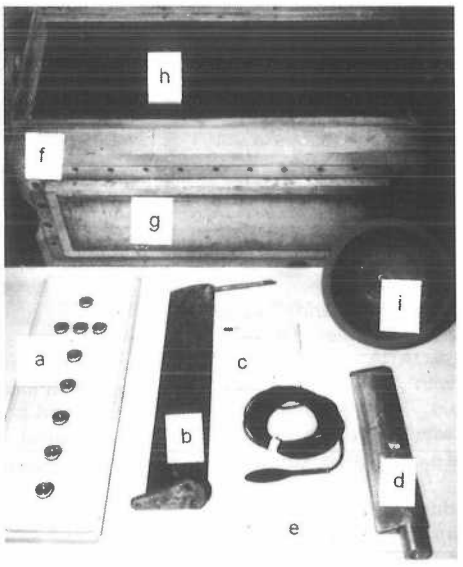

Fig. 1 **Acoustic sensors developed for the use in cavitation tunnels and towing tanks**

2.2 Reverberant method [22, 23, 26]

The acoustic field in the tunnel or the unlined chambers was found nearly reverberant, so that a simple omnidirectional sensor mounted in them simulates the integration needed in (3) and (4). By time-averaging the operation $<>_{\phi}$ is also realised, so that, after suitable calibration, the estimates of (4) are obtainable. Such a reverberant measurement method, in which sensor's and source's locations are not critical, is simple but can produce rather useful results.

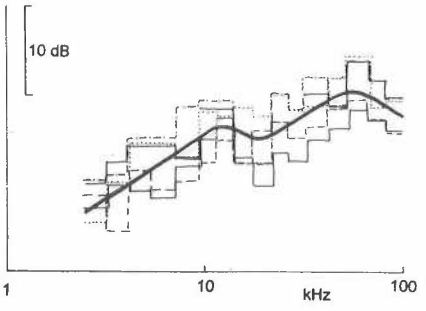

Fig. 2 **Acoustic transfer functions**

The insensitivity to source's location, which, by the reciprocity principle, implies the insensitivity to sensor's location too, is illustrated in Fig. 2. It presents some transfer functions obtained, at approximately constant air-content values, for various source locations in the unlined chambers, on the propeller disc and close to it. The actual transfer functions vary from the mean by up to 5 dB. Thus, if the mean is used for calibration, an error of up to 5 dB may occur.

Another test of the reverberant method applicability is presented in Fig. 3. Here, the four curves related to four dif-

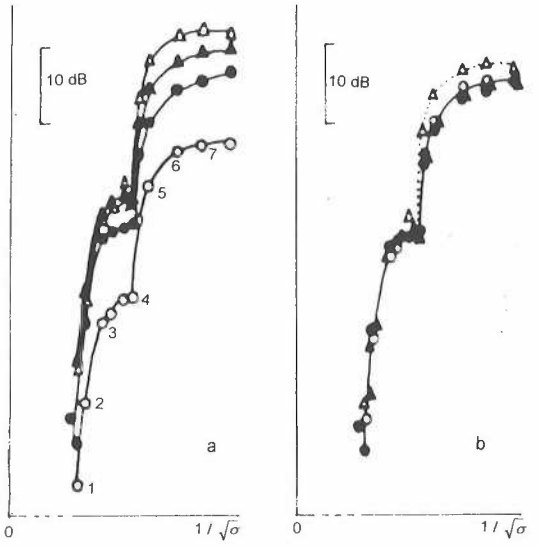

Fig. 3 **Typical cavitation noise level curves**

ferent sensor positions illustrate the dependence of the high frequency model propeller cavitation noise level on the cavitation number, $\sigma = (P - P_v)/(\rho v^2/2)$, where P is hydrostatic pressure at the propeller axis, P_v is water vapour pressure, ρ water density, and v is the circumferential speed of blade tips. The direct measurement results obtained from the same propeller by means of sensors in four locations are shown in Fig. 3a. In Fig. 3b these differences in attenuation are compensated for, so that an estimate of (4) is obtained.

The final results obtainable are also illustrated by Fig. 3. By a simple visual observation, various stages of cavitation can be assigned to the dots indicated: 1-no cavitation, 2-weak intermittent hub cavitation, 3-steady hub cavitation, 4-slightly stronger hub cavitation, intermittent tip vortex cavitation, 5-stronger hub and tip vortex cavitation, 6-strong hub and tip vortex cavitation, incipient back cavitation, and 7-strong hub and tip vortex cavitation, and cavitation across 5% of the back area.

2.3 Chambers and reflectors [15, 16, 26]

The evidence of the nearly-reverberant character of the acoustic field in a tunnel with unlined chambers is presented as **a** and **b** in Fig. 4. A broad-band omnidirectional sound was generated by a hydrophone replacing the propeller, and the acoustic pressure was picked up by the measuring sensor. This pressure, referenced to the free-field unit distance generated pressure, is shown as **a** (result of the measurement) and **b** (asymptotic theoretical model of the envelope) vs. time delay expressed as the length in meters of the path travelled by the sound directly from the emitter (**d**) or via one or more reflections off the tunnel and chambers' walls (**r**).

With the lined chambers the dependence shown as **b'** in Fig. 4 was obtained, indicating the suppression of reflections. However, only with an elliptic reflector were practically obtained free-field conditions as in Fig. 5 (**d**-direct wave, **r**-reflections, **c**-wave collected by the reflector). Fig. 6 describes the spatial resolution obtained by the reflector, and Fig. 7 its gain vs. frequency. It can be seen that, within a decimetre or so, the measurement by

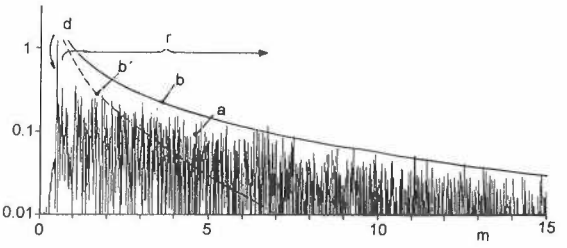

Fig. 4 **Structure of the acoustic field in the chamber**

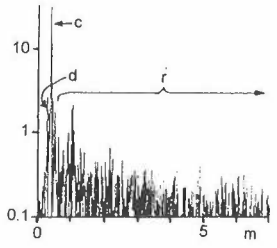

Fig. 5 **Structure of the field as sensed by the elliptic reflector**

means of such a reflector forms the basis for the results of the type (1).

The performance of the reflector was found to be highly dependent on the quality of reflecting surface geometry. Figs. 5-7 refer to the reflector made of the material known under commercial name *klegecell*. A fine-surface electromagnetic reflector with the air behind it improves the performance (better spatial resolution and a gain of 20 dB instead of 10 dB). A further gain and resolution improvement can be achieved by using two reflectors with axes crossing in the focus and multiplying or correlating their outputs.

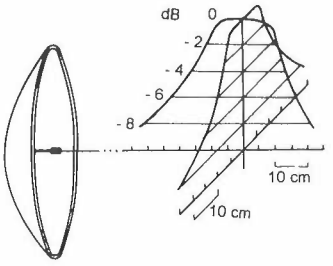

Fig. 6 **Spatial resolution of the elliptic reflector**

2.4 Space-time filtering

An operational disadvantage of the measurements with the reflector is the inconvenience of positioning it to bring the focal region to coincide with various parts of the cavitation flow. This can be avoided by another approach: signals from two or more spatially-separated sensors are processed in such a way to obtain focusing by space-time filtering.

The two-sensor correlation tracking method [8, 9, 24] is an example of such an approach which gives results of type (2), i.e. a circumferential average description of cavitation, spatially-resolved over the propeller. If the propeller operates in a homogeneous wake, an unbiased estimate is obtained, while in

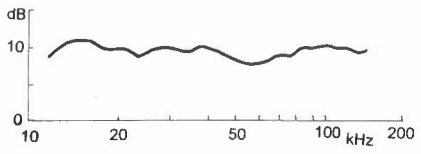

Fig. 7 **Gain of the elliptic reflector**

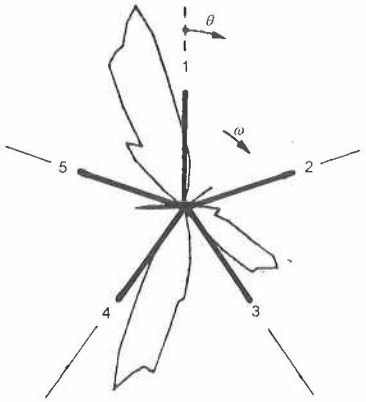

Fig. 8 **A result of the correlation tracking method (θ is in the system fixed to the propeller)**

an inhomogeneous wake a high bias error arises through the circumferential averaging. Fig. 8 illustrates the result obtained on a five-bladed propeller model in the cavitation tunnel using this method. Here the (average) angular distribution of noise sources in the propeller disc at the tip radius is given (θ - see paragraph 1; ω denotes the rotation direction). The lines indicate propeller blade positions. The propeller was operating in a homogeneous wake in a regime with an approximately identical cavitation pattern on each blade in all angular positions. However, as can be seen, noise sources were not homogeneously distributed. Obviously, strong contributions to the overall noise arise only from narrow angular intervals lying about 20° behind blades 1, 3, and 4. The contributions related to blades 1 and 4 were more pronounced than the one related to blade 3, while those of blades 2 and 5 were negligible.

2.5 Modulation analysis [5, 11, 19]

Amplitude modulation of cavitation noise of a propeller operating in an inhomogeneous wake field is a very useful source of data on cavitation. The modulation may be described by the normalised envelope waveform, $m(t)$, of the cavitation noise signal in a suitable frequency band, the normalised noise power (the square of $m(t)$), or the amplitude spectrum, $M(f)$, of $m(t)$. With a sufficiently narrow frequency band and suitable calibration, $m(t)$ produces estimates of the results of the type (3). Here, the time variable t has to be transformed into the propeller angular position ϕ, and the harmonics kn, $k = 1, 2,...$, of the propeller rotation rate, n, have to be observed in $M(f)$. By such an analysis the wake influence is most easily observed, especially if one replaces $m(t)$ by the function $<m(t)>$ obtained by averaging $m(t)$ over many periods of propeller rotation. Also, the root-mean-square value, m_o, of variations $m(t)$-1, which describes modulation depth, proves useful in the identification of various cavitation forms.

Figs. 9-11 are a set of illustrations of cavitation noise modulation analyses of some five-bladed onboard propellers. The steep rise of the m_o vs. n curve in Fig. 9, when compared with the dependence of high frequency noise level (dB) on n, shows high correlation of m_o with the onset of cavitation. This fact makes the modulation depth a useful tool for cavitation threshold determination.

Various forms of $M(f)/m(t)$ pairs are illustrated in Fig.10. In (a) the cavitation threshold has just been reached. Only one blade is cavitating within a narrow angular range; the onset is accompanied by many practically equal harmonics which start appearing from $k=1$. In more developed cavitation regimes (b,c,d), contributions also arise from other blades, emphasising

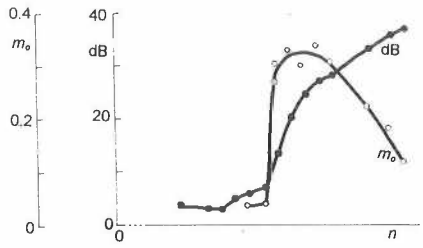

Fig. 9 **Modulation depth and noise level curves**

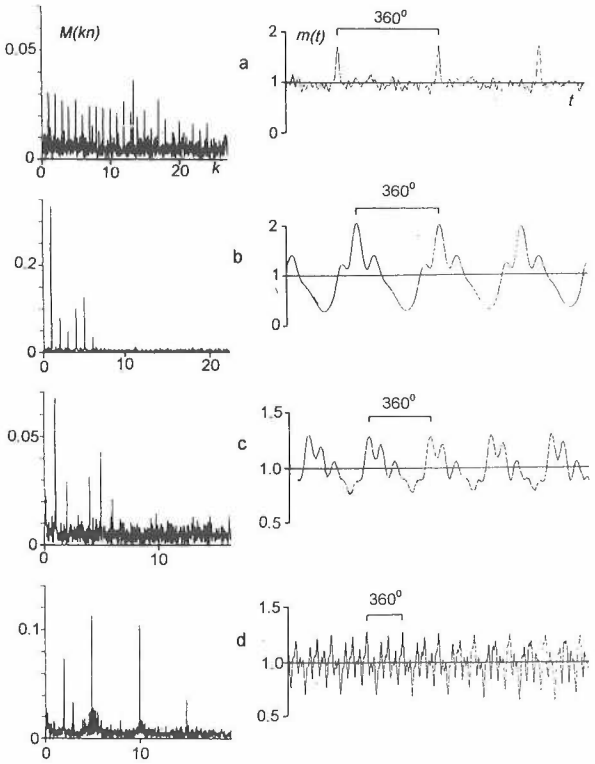

Fig. 10 **Modulation spectra and waveforms**

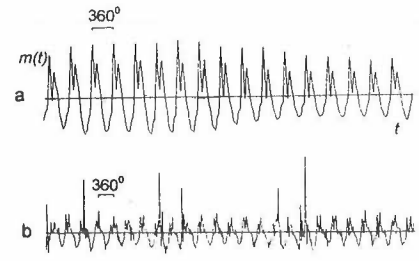

Fig. 11 **Cavitation nonstationarity detected by noise modulation**

the blade-passage rate, i.e. $k = 5, 10, 15,...$ Obviously, the modulation depth decreases. (Cf. the high-n part of the m_o curve in Fig. 9).

In contrast to Fig. 10, where stationary $m(t)$'s are shown, $m(t)$ functions given in Fig. 11 show some nonstationarity. The most probable causes are: (a) rudder deflection; (b) randomly appearing water volumes that are especially weak with respect to cavitation.

2.6 Cavitation identification

Another example of application of the modulation analysis for cavitation identification is shown in Fig. 12. Here $<m(t)>$ is drawn as a function of ϕ for several cavitation regimes of a five-bladed propeller. Just as in Fig. 8, ω denotes rotation direction. Otherwise, the two formats differ fundamentally: Fig. 8 describes cavitation distribution over the propeller itself and is related to type (2) description, while Fig. 12 shows merely how the total propeller noise depends on the propeller angular position, and is related to type (3).

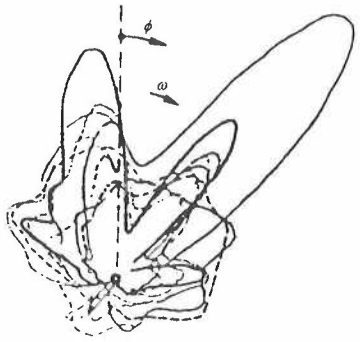

Fig. 12 **Modulation curves recorded at different σ-values (ϕ is in the system fixed to the ship hull)**

The angular distance of the two large peaks in Fig. 12, as well as their dominance, leads to the conclusion that, on this particular propeller, only one blade was strongly cavitating and that it produced (acoustically) significant cavitation at only two propeller positions in the wake field. By a more detailed analysis such issues can be quantified. Indeed, the *Blade & Wake Decomposition Technique*, proposed in [40], furnishes the circumferentially-averaged estimates of the cavitation intensity related to every propeller-blade/wake-lobe pair. This enables a combined analysis-synthesis data processing which yields results such as that given in Fig. 13 related to a five-bladed propeller operating in a wake having four distinctive cross-like lobes. Here, synthetic σ-dependencies of noise level (σ_{cr} is the critical value of σ) related to different propeller blades in a particular wake lobe, and different wake lobes as sensed by a particular blade are shown.

2.7 Air-content influence

Various methods for total air-content measurement [2, 17] and distribution analysis of free-air content of water [7, 25, 26, 43] were tested at the Brodarski Institute. The Coulter counter was found to be inapplicable in a real situation when connected to a cavitation tunnel [7, 25, 43]. Among several optical methods tried, laser beam scattering proved most useful. However, due to the non-ideal laser beam profile, raw results of analysis are loaded by a heavy bias error. To compensate for this effect a deconvolution procedure was conceived [28].

The light scattering method was used in an experiment lasting for a week, in which the air content and model propeller cavitation noise were measured in a cavitation tunnel simultaneously [33]. The propeller was operated at constant propulsion and (nominal) cavitation conditions. Water supersaturated with the air was fed into the tunnel and was gradually degassed

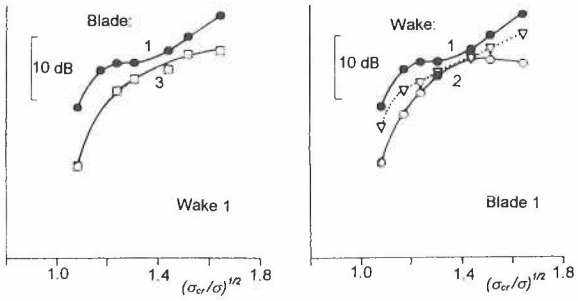

Fig. 13 **Synthetic noise level curves**

to 18% of the saturation value. Over the 5-50 kHz frequency band, the dependence of noise attenuation on the total free-air content, AC, normalised to its critical value, CAC, was consistent with a simple rule (Fig. 14). There was an abrupt fall of the

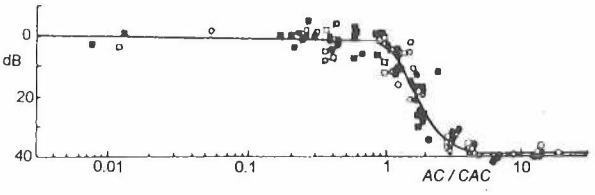

Fig. 14 **Noise attenuation due to free air in water**

noise level when AC rose above CAC, and there was virtually no change in the noise level when $AC<CAC$. There was, however, a frequency dependence of the effect: as noise frequency increased, CAC decreased (Fig. 15).

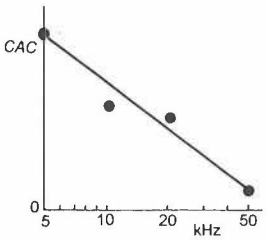

Fig. 15 **Critical air content**

To discriminate between two possible mechanisms of air content influence on cavitation noise level - damping of bubble collapse dynamics due to gas in the bubble, and the attenuated propagation of sound through the free bubbles - acoustic transmittance of bubbly water was measured in a tunnel [31, 33]. The attenuation thus obtained (Fig. 16), corresponding to high (a) and low (b) air content, is shown as a function of noise frequency and tunnel cavitation number, $\sigma_0 = (P\text{-}P_v) / (\rho v_0^2/2)$, where v_0 is the free flow velocity and the other quantities are already defined. (An increase of σ_0 is indicated by the arrows; in both figures the same range of σ_0 was covered.) The comparison of this essentially low frequency

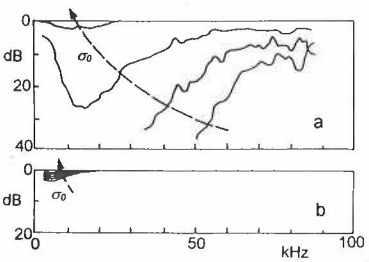

Fig. 16 **Acoustic transmittance of bubbly water**

effect with the one presented in Figs. 14/15 leads to the conclusion that, at least in the case considered, the damping of collapse dynamics was a dominant influence of air-influence.

2.8 Hydrostatic pressure influence [34, 40]

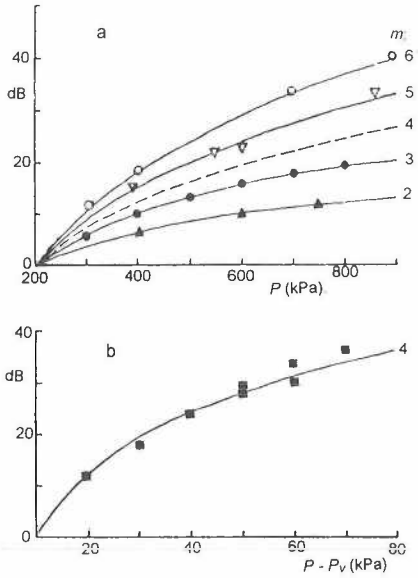

Fig. 17 **Constant-σ pressure-dependence of high frequency cavitation noise: (a) different full-scale propellers, (b) a model**

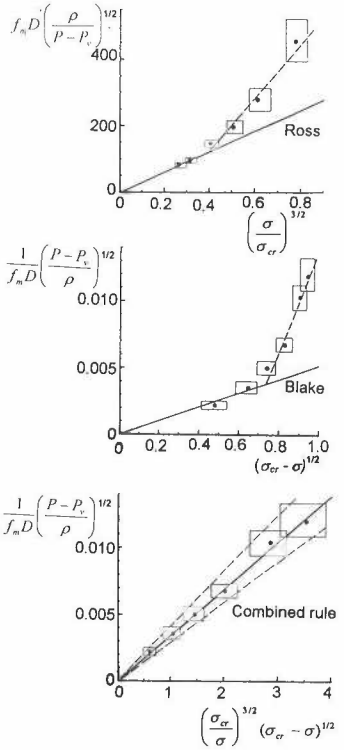

Fig. 18 **Frequency scaling rules: full-scale propeller data**

According to published data, a constant-σ power spectrum density of high frequency propeller cavitation noise has a power-dependence, the power, m, equal to 5/4 predicted theoretically [48] and 3/2 found experimentally [51]. Such a fixed, rather low value of m is also suggested by the ITTC [54]: 1.5 for the high frequency range and 1.5 to 2 for all the frequencies involved. The Brodarski Institute team had an opportunity to study the full-scale hydrostatic pressure influence over a wide range of pressure and on several different propellers. The results of such measurements, given in Fig. 17a, in which different dots represent different propellers, and Fig. 17b showing a model result, include the m-values like those above but also values as high as 6. This speaks against the idea of a fixed universally applicable m-value. There is no plausible explanation for this discrepancy between the results of the Brodarski Institute experiments and published data except that most published data were derived in experiments in which only a narrow pressure range was observed. The wide spreading of m-values may imply that there were different types of cavitation and that these different types display different constant-σ hydrostatic pressure dependencies.

2.9 Noise frequency scaling

Most often, the mean total power spectrum density of propeller cavitation, $<\Sigma\{G(f;r,\theta,z;\phi)\}_{r,\theta,z}>_{\phi} = g(f)$, is measured and studied as a function, $g(f,P,n,D)$, of the hydrostatic pressure at the propeller axis, P, propeller revolution frequency, n, and propeller diameter, D. When comparing such spectra collected at different P-values or, related to model experiments and their scaling, different D-values, a question arises of which noise frequencies should be considered related, i.e. how to scale frequency, f, in two situations. There are two cited and commonly-used but different answers to this question:

Blake [52, 53]:
$$f_m = \frac{F_B}{D}\left(\frac{P - P_v}{\rho}\right)^{1/2}\frac{1}{(\sigma_{cr} - \sigma)^{1/2}}, \qquad (5)$$

Ross [49]:
$$f_m = \frac{F_R}{D}\left(\frac{P - P_v}{\rho}\right)^{1/2}\left(\frac{\sigma}{\sigma_{cr}}\right)^{3/2}. \qquad (6)$$

Here f_m is the frequency at which the spectrum peaks, and F_B and F_R are dimensionless constants. When comparing different situations, f/f_m should be kept constant. While the two scaling rules predict the same P and D dependencies, they diverge with respect to the cavitation number. Rule (5) may be expected to function well at σ close to σ_{cr}, while (6) is most applicable for $\sigma << \sigma_{cr}$. Indeed, when applied to the full-scale data of one of the tested propellers, no arguments against these rules within their appropriate σ-ranges could be stated. However, the new *combined frequency-scaling rule* proposed in [44],

$$f_m = \frac{F_C}{D}\left(\frac{P - P_v}{\rho}\right)^{1/2}\left(\frac{\sigma}{\sigma_{cr}}\right)^{3/2}\frac{1}{(\sigma_{cr} - \sigma)^{1/2}}, \qquad (7)$$

is valid continuously over a broad σ-range (Figs. 18 and 19); here F_C is another dimensionless constant.

2.10 Noise level scaling [4, 26, 34, 40, 44]

The procedure of propeller cavitation noise scaling adopted as an internal standard of the Brodarski Institute includes the following steps:

(a) estimate the height of cavitation threshold, described by σ_{cr}, by means of the modulation depth or the level-vs.-n curve;

(b) scale frequency according to the rule (7) with the best-fit F_C;

(c) express spectra in the variable f/f_m as a function of σ, P, and D;

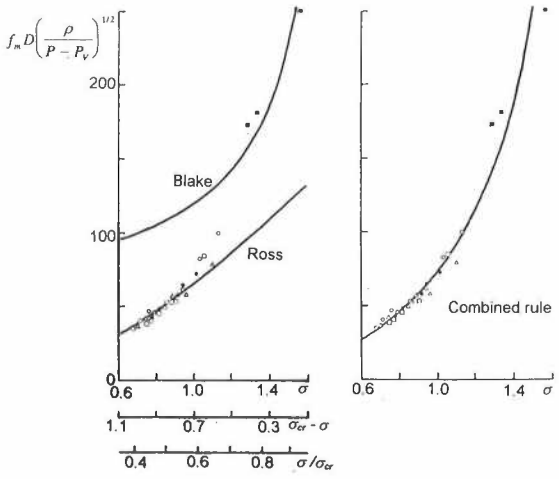

Fig. 19 **Frequency scaling rules: rotating-rod data of [47]**

(d) express the σ-dependence in the variable σ/σ_{cr}, and model the noise power spectrum density or the noise power (within a fixed band expressed in f/f_m) by

$$\text{const.} \times \left(\frac{\sigma_{cr}}{\sigma}\right)^{1/2}\left[\left(\frac{\sigma_{cr}}{\sigma}\right)^{1/2} - 1\right]^2 \qquad (8)$$

[49] for $\sigma_{cr} - \sigma << \sigma_{cr}$, and otherwise by an empirically determined function of σ/σ_{cr};

(e) express, according to subsection 2.8, the remaining dependence on P by a power-law, the power, m, being chosen for the best fit;

(f) express the D-dependence in the well-established way [48, 49].

As far as the air-content of water in model tests is concerned, only the results obtained with $AC<CAC$ (see Fig. 14) should be considered.

The steps (d) and (e) are illustrated in Figs. 20 and 21. Fig. 21 refers to pure cavitation components (background power subtracted). The dashed curves in Fig. 21 follow (8). This σ-rule proves to be good for incipient and weak cavitation.

2.11 Fouling and damage effects [21, 32]

An initially clean propeller on a ship sailing in the Adriatic Sea was monitored during a six-month period of fouling. By periodic measurements, in which the modulation-depth method was used, the dependence $n_{cr}(d)$ of the critical propeller rotation rate (the one related to the cavitation threshold), n_{cr}, on the number of days, d, after the beginning of the monitoring was obtained. Using $n_{cr}(d)$ in the function $v(n;d)$, specifying the ship speed, v, at propeller rotation rate n after d days of fouling, the critical ship speed in a given state is obtained: $v(n_{cr}(d);d)$. This yields the relative critical speed decrease vs. d:

$$\text{CSD} = \frac{v\,(n_{cr}(d);\, d) - v\,(n_{cr}(0);\, 0)}{v\,(n_{cr}(0);\, 0)}.$$

It is easy to see that there are two mechanisms producing the *CSD*: a propeller fouled to a greater extent starts to cavitate

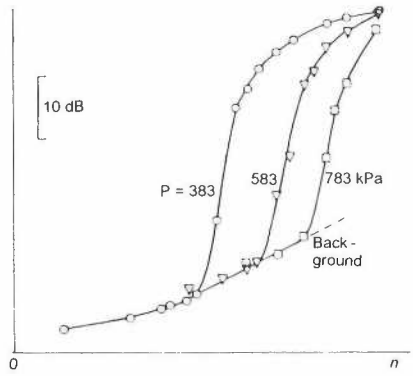

Fig. 20 **Raw measurement results**

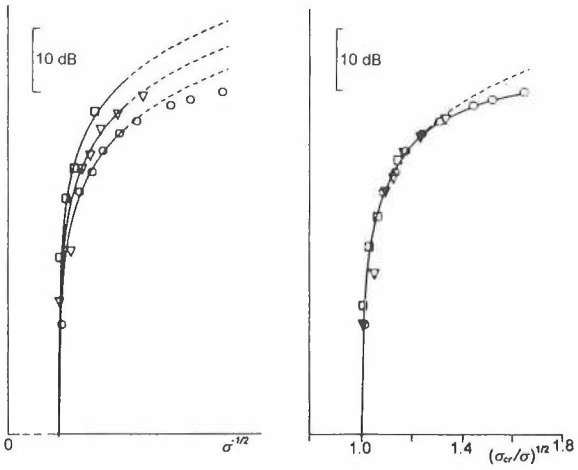

Fig. 21 **Scaling: σ (left) and explicit P-dependence (right)**

at a lower rotation rate, but the ship speed is also lower at that rate of propeller rotation. The appropriate nomenclature for the two (additive) components of the *CSD* induced by the two mechanisms is: cavitation and propulsion. The definition of the cavitation component analogous to the above total *CSD* is:

$$\frac{v\,(n_{cr}(d);\, d) - v\,(n_{cr}(d);\, 0)}{v\,(n_{cr}(d);\, 0)}.$$

In Fig. 22 the *CSD* dependencies measured as described above are presented as the total one - T and the one due to the cavitation - C.

Here, the power increase *PI*, necessary to maintain the same ship speed, is also given [50]. WS denotes transition from winter to summer, which changes the slope of the *PI* vs. d dependence.

Conclusion? A period of six months of fouling, part of which included the winter season, led to 25% lower critical ship speed. In the first months the increase of loss was rather rapid. The loss due to the cavitation component was prevalent. In contrast to the increase of power, the critical speed decrease was initially faster but tended to slow down.

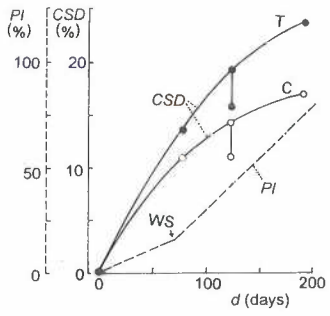

Fig. 22 **Propeller fouling log**

A case showing the effect of a damage of a propeller is described in Fig. 23. Here, high frequency cavitation noise level vs. propeller rotation rate, n, is shown for a fouled but undamaged propeller (NON) and for the same propeller after it got damaged but was cleaned (DAM). In the DAM state the blade tips were twisted by 1.5 cm towards the face at the radius where a profile length was about 15% of the propeller radius, and at higher radii. The consequences of damage are apparent: 40% lower critical propeller rate and a significant noise level increase.

2.12 Full-scale measurement procedure

In order to collect high-quality noise data for the purposes like those presented in subsection 2.9 (which requires stable and stationary data not corrupted by disturbances and representing free field of a propeller as a source), streamlined holders were used onboard a submarine to carry carefully chosen and mounted hydrophones (Fig. 24). Such a sensory set and an onboard automatic signal conditioning and acquisition system [14] complemented with a system for underwater analysis of acoustic transfer functions proved rather useful. The system for full-scale data collection, used for the issues like those in subsections 2.8-2.11 or for general ship noise assessment, included (*i*) such and similar measurements by means of hydrophones fixed to the ship hull, and (*ii*) acoustic-range measurements. In both types of measurements, (*i*) and (*ii*), far-field components were picked up. Type (*i*) yielded reliable descriptions of details of parametric dependencies, and the acoustic-range results ensured proper calibration.

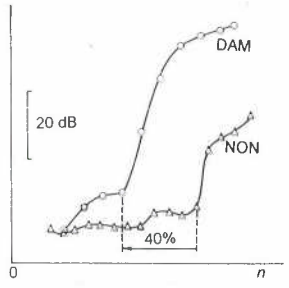

Fig. 23 **Acoustical effect of damage**

2.13 Acoustic optimisation of nozzles and ducts [38, 39]

Systematic model experiments were performed to investigate the possibilities of attenuating noise from a propeller in a nozzle or in the duct of a thruster. These experiments included (a) optimising the geometry of the nozzle/duct, (b) using a compliant lining to muffle the source, and (c) using reflective material to suppress the transmission of vibro-acoustic excitation to the ship's hull. Attenuation of up to 30 dB was found to be possible. Ways to protect the acoustically (and inevitably also mechanically) soft material were also developed.

Fig. 24 **The second author checking details before an onboard measurement**

3. Rotation noise

3.1 Water surface effect on a dipole source [12, 16, 35]

To estimate the free-field level of propeller rotation noise from the results of measurements in a towing tank or shallow sea, the acoustic influence of the boundaries has to be taken into account. Typical propeller depths are much smaller than the tank dimensions or the sea depth. Thus a simple model of the boundaries' effect seems to be appropriate - the one which accounts for the water surface influence only. The transfer function for a shallow submerged horizontal dipole source representing the propeller as a source of rotation noise, as shown in Fig. 25, confirms this assumption. Curve (a) corresponds to the simple model described above, while the dots (b) are obtained by summing many reflections from the water surface, tank bottom and walls.

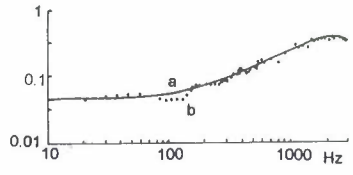

Fig. 25 **Horizontal dipole in a towing tank**

This simple dipole model was applied to the problem of onboard propeller rotation noise measurements. The model was broadened by a description of the averaging effect due to the time constant of the measuring equipment, which cannot be avoided since random fluctuations have to be suppressed.

Given the measuring hydrophone position, propeller depth, the parameter L characterising the inertia of the measuring set, and the spectral line frequency f, the resulting model describes the normalised dependence $\psi(x,L)$ of a spectral line amplitude at position x along the ship route [35] as illustrated in Fig. 26. Here the theoretical curves (smooth) are fitted to the results of the analysis carried out with three values of L. The dashed lines are estimates of the background noise which is independent of x. In the model of the rest, $A\psi(x,L)$, the constant A is adjusted

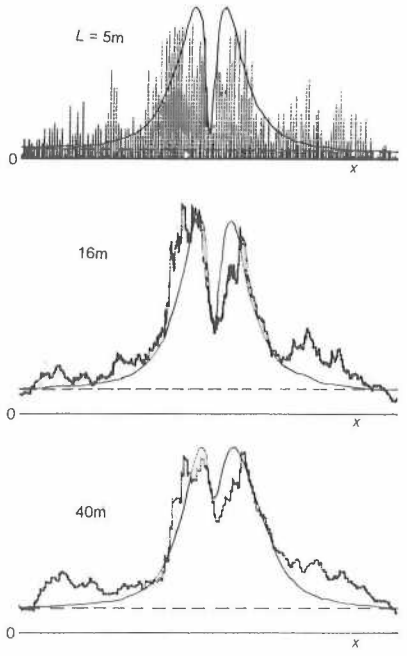

Fig. 26 **Estimation of rotation noise amplitudes**

for the best fit. In this way the line spectrum source level of the dipole source representing the propeller is determined. The reduction of the entire curve to a single numerical quantity results in an efficient suppression of random errors.

3.2 Spectral-line broadening

In a usual description of propeller rotation noise its spectrum is reduced to pure lines at the blade rate and its harmonics. According to Aleksandrov [45], cavitation generates some additional lines within this array. In our experiments no lines except for the blade-rate harmonics occurred, but the broadening of the spectral lines, which had to be attributed to cavitation, was found [6]. In Fig. 27 the experimental results related to this effect are presented. The rotation noise of a cavitating onboard propeller was analysed by means of the method presented above. The resulting amplitudes of a spectral line, centred at a frequency f_o, are shown vs. frequency f. The stability of the propeller rotation frequency was better than the resolution width of the analysis, which is equal to the separation of the neighbouring dots. A line broadening of 5% can thus be observed.

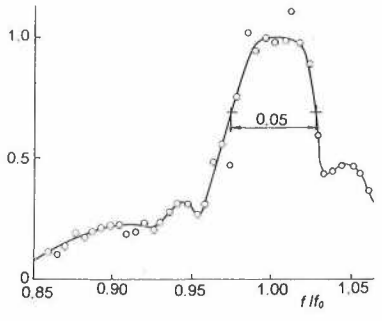

Fig. 27 **Cavitation generated broadening of rotation noise spectrum lines**

4. Propeller singing

4.1 Method for singing diagnostics [20]

A method used in the Brodarski Institute for the identification of propeller singing is presented by an example in Figs. 28-31. Low frequency noise was measured by a hydrophone located on a hull, in the vicinity of a five-bladed onboard propeller. Several values of propeller rotation rate, n, were tested. The obtained spectra are shown in Fig. 28 for three values of n normalised to the maximum n-value, n_{max}. Several strong spectral lines were found, some appearing at different values of n.

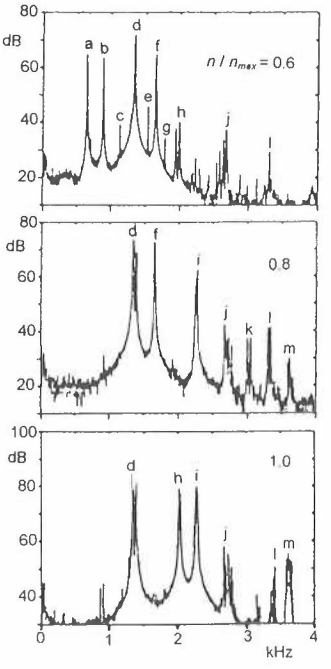

Fig. 28 **Noise spectra of a singing propeller**

To find out whether the source of the lines was located somewhere in the ship propulsion complex or was generated by the propeller, the amplitude modulation of these lines was analysed. A typical result is given in Fig. 29. Synchronisation with the shaft rotation is evident.

The next step of the procedure includes the analysis of propeller resonant frequencies. The propeller blades, still underwater but not rotating, were struck with a hammer at various positions. The resulting sound was picked up by the hydrophone and analysed. The recorded spectra (Fig. 30) display clearly resonant vibrations of the propeller. Various spectral lines are denoted by a, b, c, ... The crucial fact is the full coincidence of the line frequencies in Fig. 28 and the resonant frequencies in Fig. 30 (in the two figures the corresponding lines have the same notation).

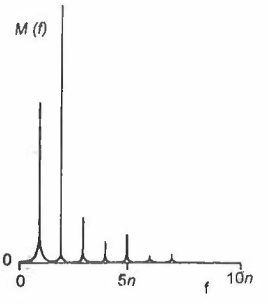

Fig. 29 **Modulation of a spectrum line**

Final evidence that propeller singing was the source of the detected noise is given in Fig. 31. Here the n-dependence of the frequencies of the propeller noise spectral lines with amplitudes higher than a suitably chosen limit value is shown. The form of dependence characteristic of singing is such that for higher values of n higher frequencies are excited, which confirms the relevance of the vortex shedding frequency for the process.

In addition, propeller vibrations were also investigated by optical means (Fig. 32).

5. Tools for scaling, prediction and optimisation

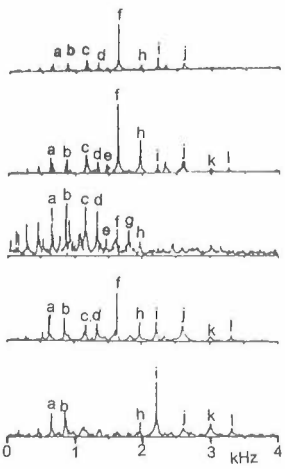

Fig. 30 **Propeller resonances**

For three noise components, the scaling rules and semi-theoretical models for prediction as well as propeller optimisation with respect to them were constructed: cavitation noise [26, 34], rotation noise [18, 30], and vortex noise [37]; there is also a tool for acoustic optimisation of nozzles and ducts [39]. These models are intended for early stages of a ship and propeller design, when only the most basic data on the propeller are available, details are still to be optimised, and the directions of changes have yet to be determined.

No way was found to scale or predict propeller singing. Only the above-presented method for diagnosis was devised, and two known ways to eliminate the singing were used: producing a propeller from a material with high internal vibration damping, and cutting the trailing blade edge in a suitable way.

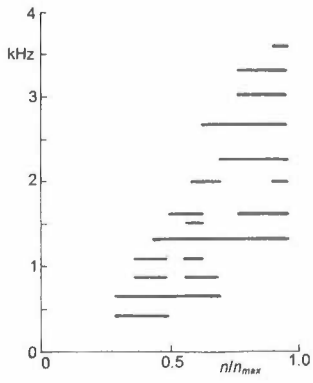

Fig. 31 **A crucial fingerprint of singing**

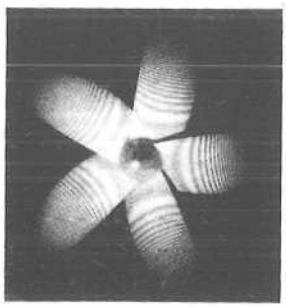

Fig. 32 **Holographic interferometry of a vibrating propeller**

Conclusions

The results of the reviewed research into propeller noise carried out at the Brodarski Institute include the following:

- Classification of measurement methods and implementation examples of each measurement type. These methods yield results ranging from reliable estimates of mean free-field spectra to details of parametric dependencies of noise, and data which enable acoustic diagnosis of propeller cavitation details.
- Discovery of a new physical effect in rotation noise of a cavitating propeller, and new findings related to the dependence of cavitation noise on hydrostatic pressure, cavitation number, and air-content.
- Experimentally proved scaling rules which, in several aspects, strongly diverge from the ones suggested by other authors.
- Quantification of the effect of propeller fouling on cavitation noise.
- Reliable method for propeller singing diagnostics.
- Analytic tools for prediction of cavitation, rotation, and vortex noise and for propeller optimisation with respect to them, suitable for use in early design stages.
- An approach to acoustic optimisation of nozzles and ducts.

Acknowledgement

The authors acknowledge the co-operation of Ivo Šemeš, Dubravko Krajina, and Alojz Grabrovec, the operators of the Brodarski Institute cavitation tunnels, and the crews of the many screw-propelled vessels used as platforms for field experiments. They gratefully acknowledge the continuous critical attention paid to their activity by Ivo Antunović, hydrodynamicist, and the support rendered by the project managers Branko Ryšlavy, Davorin Kajić, Ivan Mušterić, and Dušan Patarić, all with the Brodarski Institute during this research.

Bibliography*

[1] BAJIĆ, B.: "On cavitation noise spectra" (in Croatian), Elektrotehnika, 15(1972)1, p. 34-35.

[2] BAJIĆ, B.: "Optimisation of the total air-content in water measurement by means of the Van Slyke apparatus" (in Croatian), Naučno-tehnički pregled, 22(1972)8, p. 37-60.

[3] BAJIĆ, B.: "Two examples of acoustical diagnosis of cavitation phenomena on full-scale propellers" (in Croatian), Brodogradnja, 25(1974)3-4, p. 285-291.

[4] BAJIĆ, B.: "An introductory empirical approach to screw propeller cavitation noise modelling", Acustica, 33(1975)4, p. 281-285.

[5] BAJIĆ, B.: "An example of the acoustical diagnosis of the ship screw propeller cavitation", International Conference on Monitoring Diagnosis in Industry, Prague, Czech Republic, 1975, Proc., Vol. 1, p. 109-118.

[6] BAJIĆ, B.: "On the rotational noise spectrum of the cavitating screw-propeller", Acoustical Letters, 1(1977), p. 73-78.

[7] JOVANOVIĆ, I.: "On the application of the Coulter counter for measurement of the size of gas bubbles in fluid" (in Croatian), Symposium JUREMA, Zagreb, 1977, Proc., Vol. 1, Paper B15.

[8] BAJIĆ, B., and JOVANOVIĆ, I.: "Correlation method for measurement of rotating sources of noise waves - Experimental verification" (in Croatian), Elektrotehnika 20(1977)2, p. 87-94.

[9] BAJIĆ, B.: "A correlation measurement method for rotating sources of noise", Acustica, 44(1980)3, p. 161-172.

[10] BAJIĆ, B., and TASIĆ, J.: "Measurement and analysis of hydroacoustic transfer functions of a cavitation tunnel" (in Croatian), Elektrotehnika, 23(1980)1, p. 5-11.

* TPS stands for the Symposium "Theory and Practice of Shipbuilding" organised biannually at various places in Croatia.

[11] BAJIĆ, B., and TASIĆ, J.: "Cavitation noise modulation as a means for diagnosing mechanisms of propeller cavitation" (in Croatian), Elektrotehnika, 23(1980)3, p. 141-145.

[12] BAJIĆ, B., and TASIĆ, J.: "On acoustical characteristics of towing tanks" (in Croatian), 4th TPS, Opatija, Croatia, 1980, Proc., Vol. 2, p. 12.44-12.52.

[13] DŽUBUR, A.: "Laser anemometry: Principle and possibilities" (in Croatian), 4th TPS, Opatija, Croatia, 1980, Proc., Vol. 2, p. 12.62-12.72.

[14] JOVANOVIĆ, I.: "Calculator-based system for complex vibro-acoustic research" (in Croatian), Elektrotehnika, 23(1980)3, p. 147-150.

[15] DŽUBUR, A., and JOVANOVIĆ, I.: "Sensors and materials for hydrodynamic acoustics measurements", 10th International Congress on Acoustics, Sydney, Australia, 1980 (see also: Elektrotehnika (in Croatian), 23(1980)3, p. 151-156).

[16] BAJIĆ, B., and TASIĆ, J.: "On the transfer functions of the hydrodynamic tanks and tunnels with acoustic chambers", 10th International Congress on Acoustics, Sydney, Australia, 1980.

[17] KELENC, D.: "Instruments for total air-content measurement in a cavitation tunnel" (in Croatian), Naučno-tehnički pregled, 31(1981)3, p. 52-56.

[18] BAJIĆ, B., and DŽUBUR, A.: "Naive model of the ship screw propeller rotational noise spectrum", Teorijska i primjenjena mehanika, 1982, No. 7, p. 11-19 (also: 10th International Congress on Acoustics, Sydney, Australia, 1980).

[19] BAJIĆ B., TASIĆ, J., and JOVANOVIĆ, I.: "An example of acoustical diagnosis of on-board propeller cavitation noise" (in Croatian), 5th TPS, Split, Croatia, 1982, Proc., Vol. 2, p. 6.10-6.21.

[20] BAJIĆ, B., DŽUBUR, A., and TASIĆ, J.: "A case study of propeller singing" (in Croatian), 5th TPS, Split, Croatia, 1982, Proc., Vol. 2, p. 6.22-6.29.

[21] DŽUBUR, A.: "Monitoring onboard propeller cavitation and fouling" (in Croatian), 5th TPS, Split, Croatia, 1982, Proc., Vol. 2, p. 6.30-6.38.

[22] BAJIĆ, B., DŽUBUR, A., JOVANOVIĆ, I., TASIĆ, J., KELENC, D., KLAK, S., and PAVIĆ, G.: "Methods of propeller cavitation noise investigation in the Brodarski Institute cavitation tunnel No. 2" (in Croatian), 5th TPS, Split, Croatia, 1982, Proc., Vol. 2, p. 6.39-6.50.

[23] TASIĆ, J., and BAJIĆ, B.: "Test measurements of model propeller cavitation noise in Brodarski Institute" (in Croatian), 5th TPS, Split, Croatia, 1982, Proc., Vol. 2, p. 6.51-6.60.

[24] JOVANOVIĆ, I.: "Distribution analysis of cavitation noise sources across a propeller disc: A preliminary test" (in Croatian), 5th TPS, Split, Croatia, 1982, Proc., Vol. 2, p. 6.61-6.68.

[25] DŽUBUR, A.: "Methods for cavitation nuclei size distribution analysis in Brodarski Institute" (in Croatian), 5th TPS, Split, Croatia, 1982, Proc., Vol. 2, p. 6.76-6.84.

[26] BAJIĆ, B., TASIĆ, J., DŽUBUR, A., and JOVANOVIĆ, I.: "Methodology of propeller model cavitation noise testing in Zagreb Brodarski Institute", Brodogradnja, 31(1983)6, p. 329-338.

[27] BAJIĆ, B.: "A review of the theory of sound generation in fluid" (in Croatian), Naučno-tehnički pregled, 33(1983)6, p. 54-66.

[28] BAJIĆ, B.: "Deconvolution of the instrumental function to enhance the analysis of spherically symmetric particles by means of laser scattering - Mathematical model construction" (in Croatian), Naučno-tehnički pregled, 34(1984)7, p. 30-38.

[29] BAJIĆ, B., TASIĆ, J., DŽUBUR, A., and JOVANOVIĆ, I.: "Propeller noise: Some topics from the activities of Brodarski Institute", 2nd International Symposium on Shipboard Acoustics, The Hague, The Netherlands, 1986, Proc., Vol. 1, p. 91-102.

[30] BAJIĆ, B.: "KMUKAČ - Model of rotational spectrum for optimisation of screw propeller in the early stage of design (Non-cavitational regime)" (in Croatian), Brodogradnja, 34(1986)4-5, p. 219-225.

[31] TASIĆ, J.: "An investigation of sound attenuation in cavitation tunnel water caused by free air content" (in Croatian), 7th TPS, Pula, Croatia, 1986, Proc., Vol. 3, p. 5.210-5.219.

[32] BAJIĆ, B., and DŽUBUR, A.: "On the influence of fouling and damage on propeller cavitation noise" (in Croatian), 7th TPS, Pula, Croatia, 1986, Proc., Vol. 3, p. 5.239-5.245.

[33] BAJIĆ, B., TASIĆ, J., DŽUBUR, A., and DONESKI, R.: "On the influence of the gas content of water on the screw propeller cavitation noise", Acustica, 63(1987)2, p. 143-146.

[34] BAJIĆ, B.: "Quasi-theoretical model for prediction of cavitation noise spectrum of a ship screw propeller (Model construction)" (in Croatian), Brodogradnja, 35(1987)2-3, p. 87-93.

[35] BAJIĆ, B.: "Sea surface influence in full-scale measurements of rotational noise of a screw propeller" (in Croatian), Naučno-tehnički pregled, 37(1987)2, p. 34-37.

[36] BAJIĆ, B.: "Hydrodynamical acoustics is a part of hydrodynamics" (in Croatian), Round-Table Conference: Hydrodynamics in Ship Design, Zagreb, Croatia, 1987, Proc., p. 292-295.

[37] BAJIĆ, B.: "Simple model of the vortex noise of a ship screw propeller" (in Croatian), Brodogradnja, 36(1988)1-2, p. 17-22.

[38] JOVIĆ, C.: "The influence of nozzle geometry on the screw propeller acoustic field" (in Croatian), ETAN in Marine Symposium, Zadar, Croatia, 1988, Proc., p. 347-350.

[39] BAJIĆ, B., DŽUBUR, A., JOVIĆ, C., SAJE, Z., DONESKI, R., and BARIĆ, D.: "Hydroacoustical experiments on ship screw propeller nozzle and thruster tunnel models", 13th International Congress on Acoustics, Belgrade, Yugoslavia, 1989, Proc., Vol. 4, p. 439-442.

[40] BAJIĆ, B., and TASIĆ, J.: "Analysis of cavitation noise of an onboard propeller", International Symposium on Propulsors and Cavitation, Hamburg, Germany, 1992, Proc., Vol. 1, p. 215-223.

[41] BAJIĆ, B.: "Flow-induced signal decorrelation", 14th International Congress on Acoustics, Beijing, China, 1992, Proc., Paper L4.4.

[42] RADANOVIĆ, B., ŠTIMAC, T., KOMEŠTIK, V., SVILAR, D., BAJIĆ, B., SOMEK, B., and PALJAN, D.: "Acoustical measurements in laboratories of Brodarski In-

stitute, Faculty of Electrical Engineering, and Rade Končar Institute" (in Croatian), 37th Korema Conference, Zagreb, Croatia, 1992, Proc., p. 231-235.

[43] DŽUBUR, A., BAJIĆ, B., and JOVANOVIĆ, I.: "On the applicability of the Coulter counter to the cavitation nuclei size distribution analysis", International Shipbuilding Progress, 40(1993)422, p. 155-162.

[44] BAJIĆ, B., and TASIĆ, J.: "A wide sigma-range rule for frequency scaling of propeller cavitation noise spectra", Acustica, 80(1994)1, p. 50-57 (also: 2nd International Symposium on Propeller and Cavitation, Hangzhou, China, 1993, Proc., p. 236-241).

Additional references

[45] ALEKSANDROV, I.A.: "Physical nature of the rotation noise of ship propellers in the presence of cavitation", Sov. Phys. - Acoustics, 8(1962), p. 23-28.

[46] URICK, R.J.: "Principles of underwater sound for engineers", McGraw-Hill, 1967, Ch.10.

[47] LESUNOVSKII, V.P., and KHOKHA, Yu.V.: "Characteristics of the noise spectrum of hydrodynamic cavitation on rotating bars in water", Sov. Phys. - Acoustics, 14(1968), p. 474-478.

[48] MINIOVICH, I.YA., PERNIK, A.D., and PETROVSKII, V.S.: "Hydrodynamical sources of sound" (in Russian), Sudostroenie, 1972, p. 49.

[49] ROSS, D.: "Mechanics of underwater noise", Pergamon Press, 1976, Ch. 7 and 8, p. 255, 258.

[50] ANTUNOVIĆ, I.: "Survey of hull and propellers fouling effects on power required to maintain continuous ship speed" (in Croatian), Ship Trials Symposium, Zagreb, Croatia, 1980, Proc., p. 11.1-11.12.

[51] LØVIK, A.: "Scaling of propeller cavitation noise. Noise Sources in Ships - I: Propellers", Final report from a Nordic co-operative project: Structure borne sound in ships from propellers and Diesel engines, Ed. by A.C.Nilsson and N.P.Tyvand, Nordforsk, Miljovardsserien, 1981:2, Paper D.

[52] BLAKE, W.K.: "Propeller cavitation noise: The problems of scaling and prediction", 2nd International Symposium on Cavitation and Multiphase Flow Noise, Am. Soc. Mech. Engrs., 1986, Proc., p. 89-99.

[53] BLAKE, W.K., HEMINGWAY, H., and MATHEWS, T.C.: "Two phase flow noise", Noise-Con 88, Purdue University, West Lafayette, Indiana, 1988, Proc., p. 167-172.

[54] *** "Report of the Cavitation Committee", 19th International Towing Tank Conference, Madrid, Spain, 1990, Proc., Vol. 1, p. 211-213.

Addendum

In the nineties, the first author continued research into acoustics of cavitation with a new, non-military task: vibroacoustic diagnostics of erosive cavitation in hydro turbines and other hydraulic machinery. The results are presented in Internet (http://home.t-online.de/home/bajic) and in the following publications:

[55] BAJIĆ, B., and KELLER, A.: "Spectrum normalization method in vibro-acoustical diagnostic measurements of hydroturbine cavitation", Transactions of the ASME - Journal of Fluids Engineering, 118(1996)4, p. 756-761 (also: International Symposium on Cavitation CAV'95, Deauville, France, 1995, Proc., p. 7-13).

[56] BAJIĆ, B.: "Vibro-acoustical diagnosis of hydroturbine cavitation: Some measurement and analysis methods", Conference Modelling, Testing & Monitoring for Hydro Powerplants II, Lausanne, Switzerland, 1996, Proc., p. 169-178.

[57] BAJIĆ, B.: "A practical approach to vibroacoustical assessment of turbine cavitation", The International Journal on Hydropower & Dams, 3(1996)6, p. 45-50.

[58] BAJIĆ, B.: "Inflow decomposition: A vibroacoustical technique to reveal details of hydroturbine cavitation", Conference on Hydropower into the Next Century, Portoroz, Slovenia, 1997, Proc., p. 185-196.

[59] BAJIĆ, B.: "Vibro-acoustical diagnostics of hydroturbine cavitation", A2 - Science and Technology in the Alps-Adriatic Region, No. 10, 1997, p. 10-12.

[60] BAJIĆ, B.: "Ein praktischer Ansatz zur vibroakustischen Beurteilung der Kavitation von Wasserturbinen", Wasserwirtschaft, 88(1998)1, p. 26-31.

[61] BAJIĆ, B.: "Would turbine uprating be allowable with respect to cavitation? - An example of vibroacoustic diagnosis", Third International Symposium on Cavitation, Grenoble, France, 1998, Proc., p. 359-362.

[62] BAJIĆ, B.: "Transfer path tracing: A vibroacoustic technique to identify cavitation mechanisms", accepted for Conference Modelling, Testing & Monitoring for Hydro Powerplants III, Aix-en-Provence, France, 1998.

[63] BAJIĆ, B.: "Novel vibroacoustic techniques foor diagnosis ef erosive cavitation in hydro turbines", accepted for International Conference on Erosive and Abrasive Wear (incorporating ELSI IX), Cambridge, Great Britain, 1998.